Pharm Res (2011) 28:22–30
DOI 10.1007/s11095-010-0174-y

RESEARCH PAPER

Transdermal Delivery of Macromolecules Using Solid-State Biodegradable Microstructures

Janet R. Wendorf • Esi B. Ghartey-Tagoe • Stephen C. Williams • Elena Enioutina • Parminder Singh • Gary W. Cleary

Received: 1 April 2010 / Accepted: 13 May 2010 / Published online: 10 June 2010

ABSTRACT

Purpose The purpose of this work is to demonstrate the feasibility of using a proprietary technology called MicroCor™, based on solid-state, biodegradable microstructures (SSBMS), for transdermal delivery of macromolecules.

Methods The proteins FITC-BSA (66 kDa) and recombinant protective antigen (rPA; 83 kDa) were incorporated into SSBMS arrays using a mold-based, liquid formulation casting and drying process. Arrays were applied to the skin with a custom applicator and then inspected to assess the extent of microstructure dissolution. *In vitro* FITC-BSA delivery to human cadaver skin was visualized using light and fluorescence microscopy and quantified by extracting and measuring the fluorescently labeled protein. rPA-containing SSBMS arrays were applied *in vivo* to Sprague-Dawley rats. The resulting serum IgG response was measured by ELISA and compared with responses elicited from intramuscular (IM) and intradermal (ID) routes of administration.

Results FITC-BSA and rPA SSBMS arrays successfully penetrated the skin. Microstructure dissolution was observed over >95% of the array area and >75% of the microstructure length. FITC-BSA delivery correlated with protein content in the formulations. Antibody titers after transdermal delivery of rPA were comparable or higher than IM and ID titers.

Conclusions Transdermal delivery of macromolecules can be conveniently and effectively accomplished using the MicroCor technology.

KEY WORDS rPA · vaccine · transdermal · macromolecules · solid state biodegradable microstructures

ABBREVIATIONS

SSBMS	solid-state biodegradable microstructures
FITC-BSA	fluorescein isothiocyanate—bovine serum albumin
rPA	recombinant protective antigen (*ex. Bacillus anthracis*)
ID	intradermal
IM	intramuscular
IgG	immunoglobulin G
PET	polyethylene terephthalate

INTRODUCTION

The development of convenient, non-invasive, safe, efficient and effective delivery methods for macromolecules by non-parenteral administration routes continues to be an objective for a number of academic institutions and commercial organizations. Transdermal delivery of drugs is generally limited to small and potent molecules using conventional patch technology and passive diffusion mechanisms. Large molecular-weight drugs or macromolecules are generally administered by the traditional needle and syringe or, more recently, using sophisticated pen injector devices. There is a universal fear and pain component involved in needle-based drug delivery that can make the experience of therapy rather unpleasant. This "needle-phobia" is one of the major reasons for therapy non-

J. R. Wendorf · E. B. Ghartey-Tagoe · S. C. Williams · P. Singh · G. W. Cleary (✉)
Corium International, Inc.
235 Constitution Drive
Menlo Park, California 94025, USA
e-mail: gary@coriumtech.com

E. Enioutina
Department of Pathology, University of Utah School of Medicine
Salt Lake City, Utah 84132, USA

compliance, which can lead to less-than-optimal treatment outcomes. Therapy non-compliance also contributes significantly to direct and indirect economic burdens on the patient and the healthcare system.

Another limitation of macromolecule drugs is their inherent instability in a liquid state at room temperature. Most macromolecule drugs must be stored under refrigerated conditions for their intended shelf-life. This requires special manufacturing, transport and storage requirements which create additional burdens and costs to the manufacturers, healthcare providers and patients. The potential for accidental needle-stick and the resulting cross-contamination as well as the need for trained professionals to administer the injections are some of the other main obstacles with needle-based drug delivery. Several novel non-invasive technologies are currently being explored as alternatives to a needle injection for the delivery of macromolecules.

The use of microstructure-based devices for transdermal delivery of small organic molecules, peptides, proteins and vaccines has been extensively reviewed in the literature [1–3]. These devices have been fabricated from a number of materials ranging from silicon dioxide to thermoplastics and water-soluble polymers, as either solid or hollow microstructures and in numerous geometries (e.g., varying shape, height, angle, aspect ratio, etc.) [4–8]. A more elegant approach to microstructure-based devices is to incorporate the drug directly into a biocompatible and biodegradable polymer matrix and then fabricate the microstructures to be capable of skin penetration under a slight external force. Corium has developed such a technology called MicroCor, which uses solid-state biodegradable microstructures (SSBMS) that, when applied to the skin under an external force, penetrate the *stratum corneum* barrier layer of the skin and release the drug for local or systemic uptake. The SSBMS can be formulated and designed to achieve a range of drug delivery profiles, from a rapid, bolus-type delivery to a more sustained and continuous delivery.

In the studies described herein, we evaluated the potential for transdermal delivery of macromolecules using our proprietary MicroCor technology. Preliminary feasibility studies were conducted using fluorescently labeled bovine serum albumin to evaluate the functionality of the technology. To demonstrate the efficacy of the technology, antibody responses to the recombinant protective antigen from *Bacillus anthracis* (rPA) transdermally delivered using MicroCor were compared to the responses achieved after intramuscular (IM) and intradermal (ID) administration in an *in vivo* rat model. These studies highlight the special promise of the transdermal route of administration for convenient, non-invasive, safe and effective delivery of therapeutic macromolecules.

MATERIALS AND METHODS

SSBMS Design and Fabrication

The SSBMS used in this study were arranged in a hexagonal pattern at a density of approximately 700 microstructures/cm² to form an array of six-sided, pyramid-shaped microstructures with heights of 200 μm and center-to-center spacing of 400 μm. SSBMS arrays were fabricated from liquid formulations containing the macromolecules of interest as described below.

rPA-Containing Formulations

Recombinant protective antigen from *Bacillus anthracis* (rPA) was obtained from List Biologicals (Campbell, CA). The rPA was reconstituted with water and desalted using Pierce Zeba Spin Desalting columns (ThermoScientific, Rockford, IL). The desalted antigen solution was then aliquoted at three dose strengths and lyophilized. To make the SSBMS arrays, these dried rPA aliquots were reconstituted in 5 mM phosphate buffer (pH7.4, Sigma Aldrich, St. Louis, MO) containing USP grade polyvinyl alcohol, MW ~ 100,000 (PVA) (Spectrum Chemicals, Gardena, CA), trehalose (Sigma Aldrich), maltitol (Sigma Aldrich), and hydroxypropyl-β-cyclodextrin (HP-β-CD) (Cargill, Minneapolis, MN). Table I shows the individual compositions of the three different rPA formulations and the final rPA content (2.5, 5, and 10% of solids content (w/w)) after reconstitution in the polymer/excipient solution.

FITC-BSA-Containing Formulations

Fluorescein isothiocyante-tagged bovine serum albumin (FITC-BSA) was obtained from Sigma Chemical (St. Louis, MO) and reconstituted at the same dosage strengths and in the same liquid polymer/excipient solution used to make the rPA-containing Formulations II and III (Table I). The compositions of the two FITC-BSA formulations, A and B, are listed in Table II. SSBMS arrays made from these two formulations were used to quantify *in vitro* FITC-BSA delivery into the skin. Some SSBMS arrays were prepared

Table I Composition of rPA-Containing Formulations (percentage of solids, w/w)

Component	Formulation I	Formulation II	Formulation III
rPA	2.5%	5%	10%
PVA	20%	20%	20%
Trehalose	31%	30%	28%
Maltitol	31%	30%	28%
HP-β-CD	15.5%	15%	14%

Table II Composition of FITC-BSA-Containing Formulations (percentage of solids, w/w)

Component	Formulation A	Formulation B
FITC-BSA	5%	10%
PVA	20%	20%
Trehalose	30%	28%
Maltitol	30%	28%
HP-β-CD	15%	14%

from formulations containing 25% FITC-BSA with PVA, trehalose, and maltitol solely for microscopic applications. The higher FITC-BSA content of these arrays made it easier to view the microstructures and the skin penetrations under UV conditions.

SSBMS Fabrication

The SSBMS arrays prepared from both the rPA and the FITC-BSA-containing formulations were fabricated using the same method. Approximately 50 μl of formulation were pipetted and spread over the surface of a silicone mold that was cast to form a female replica of the microstructure array. The formulation was then pressurized for 10 min and dried at 32°C for 1 h. Next, approximately 100 μl of a Eudragit® E PO solution (Degussa, now Evonik Industries, Parsippany, NJ), 20% in a 3:1 ethanol:isopropanol solution, were pipetted on top of the dried rPA or FITC-BSA-containing layer, pressurized for 2 min, and then dried at 32°C for 1 h. The SSBMS array was then demolded using double-sided adhesive tape laminated to a thin sheet of polyester (PET) film. Finally, the arrays were packaged with desiccant in a heat-sealed barrier foil pouch and stored under refrigerated conditions. To verify the microstructure quality, the SSBMS arrays were inspected on a stereoscope, and only arrays with greater than 95% intact microstructures were used in the *in vitro* and *in vivo* studies.

A solid-state dry film without microstructures was fabricated as a control for the rPA immunogenicity study using rPA Formulation III. Ten microliters of the formulation were dispensed onto a PET release liner, spread to form an approximately 1″×1″ thin layer, and then dried at 32°C for 30 min. A 20 μl layer of Eudragit solution (20% in 3:1 ethanol:isopropanol) was dispensed over the dried formulation, spread to form a thin layer within the boundaries of the formulation layer, and dried at 32°C for 30 min. The solid-state film was then delaminated from the liner using double-sided tape and PET film.

The integrity of rPA after being processed into SSBMS arrays and solid-state films was verified using SDS-PAGE gel analysis. SSBMS arrays for each formulation, solid-state films, and their associated liquid casting solutions were analyzed and found to be consistent with a stock rPA standard solution, thus indicating that rPA is stable during SSBMS processing (data not shown).

SSBMS Skin Insertion Method

To insert the microstructures into the skin, SSBMS arrays were applied using the custom-made spring-loaded impactor device shown in Fig. 1. This device was developed as a research tool and was designed to generate a high velocity impact to facilitate microstructure insertion into the skin. The device is set by compressing and locking the spring in place. The SSBMS array is then attached to the tip of the impactor, and the device is activated on the skin by releasing the compressed spring. The microstructures are held in the skin by continuing to physically hold the impactor on the skin after activation. The velocity of the tip on impact against the skin was measured to be approximately 9 m/s using high-speed video analysis (ProAnalyst®, Xcitex, Inc., Cambridge, MA).

In Vitro FITC-BSA Skin Delivery Studies

SSBMS arrays made from FITC-BSA formulations were evaluated *in vitro* for skin penetration efficiency and FITC-BSA delivery using split-thickness human cadaver skin (New York Firefighter's Skin Bank, New York, NY). The arrays were die-cut into 16 mm diameter discs and applied to the skin for 2 min using the spring-loaded impactor device. SSBMS arrays and the skin were photographed using light and fluorescence (UV excitation) microscopy to visualize the dissolved microstructures and the microstructure penetrations into the skin. The treated skin was tape-stripped three times to remove any residual FITC-BSA left on the surface of the skin. To quantify the amount of FITC-BSA delivered with Formulations A and B, skin sites (n=8 per formulation) were excised and incubated in 1 ml phosphate-buffered saline (PBS, Sigma) supplemented with

Fig. 1 Photograph of custom-made spring-loaded impactor used for applying SSBMS arrays to skin in *in vitro* and *in vivo* studies.

2% sodium dodecyl sulfate (SDS, Sigma Aldrich) to extract FITC-BSA from the skin. Skin extractions were performed for 24 h at room temperature on an orbital shaker (200 rpm). The solution extracts were analyzed for FITC-BSA content using a fluorescence microplate reader (SpectraMax M5, Molecular Devices, Sunnyvale, CA). The standard curve range was 0.05–25 μg/ml, and excitation and emission wavelengths used to detect the FITC label were 494 nm and 525 nm, respectively.

In Vivo rPA Delivery and Immunization Study

Animals

Female, Sprague-Dawley Rats (approximately 220 g) from Charles River (Wilmington, MA) were chosen because they were the smallest animal model compatible with the size of the SSBMS arrays (16 mm diameter) and the method of array application. Animals were anesthetized with halothane during skin site preparation procedures, prior to injection and MicroCor immunizations, and during bleeds. To achieve longer anesthesia times for the MicroCor treatments, ketamine/xylazine (9:1) was also administered. All animal husbandry and handling procedures were performed in accordance with approved IACUC procedures.

Study Design

Each animal received a primary IM injection immunization on Day 0 followed by a second ID, IM, or transdermal immunization using SSBMS on Day 28 as described in the overall study design in Table III. Five animals were assigned to each treatment group.

Preparation of IM and ID Formulations

To prepare the primary immunization liquid formulation for the intramuscular (IM) and intradermal (ID) administrations, rPA was mixed with 1X phosphate-buffered saline containing 2 mg/ml of aluminum hydroxide adjuvant (alum) (Alhydrogel, Accurate Chemical, Westbury, NY) for a final concentration of 10 μg rPA per 100 μl dose. For the second immunization, the three liquid formulations were prepared in 1X phosphate-buffered saline with no alum to final concentrations that yielded 1 μg rPA per 50 μl intradermal dose (Group 2), 10 μg rPA per 50 μl intradermal dose (Group 3), or 10 μg rPA per 100 μl intramuscular dose (Group 4). All liquid formulations were freshly prepared on the day of immunization and used within four hours of preparation.

Animal Immunizations

For the ID injections, the anesthetized rats were shaved to allow for visualization of the site of application. The study staff observed that all ID injections yielded a blister, approximately 5 mm in diameter, consistent with tissue separation at the epidermal/dermal junction, thus confirming successful ID injection. Shaving was not required for the IM injections, which were performed in the thigh.

For the transdermal (SSBMS) and solid-state film groups, the anesthetized rats were clipped and shaved with an electric razor to remove the hair on the left flank. The site was washed with water-soaked gauze, allowed to air dry for 15 min, and then examined under a white light to verify that the skin was free of hair and any visible nicks or scratches. The solid-state film or the SSBMS array were each die-cut into 16 mm diameter discs and attached to the tip of the preset spring-loaded impactor. The impactor device was then activated and held *in situ* for 2 min on a flap of flank skin to apply the test articles. To assess the application sites for local skin tolerability, each skin site was photographed and scored for edema and erythema using the 0 (none) to 4 (severe) scale of the Draize scoring system within 15 min of removing the device [9].

Blood samples were obtained from all animals before immunizations to establish a baseline IgG antibody level. On Day 0, each rat received the primary immunization of 10 μg rPA with adjuvant delivered via a 100 μl IM injection. Blood was drawn two weeks (Day 14) after this injection, and the serum, isolated by centrifugation of the

Table III rPA Immunization Study Design

Group	Animals	Immunization 1 Day 0	Immunization 2 Day 28
1	5	Liquid, IM 10 μg rPA, Alum	None
2	5	Liquid, IM 10 μg rPA, Alum	Liquid, ID 1 μg rPA, no Alum
3	5	Liquid, IM 10 μg rPA, Alum	Liquid, ID 10 μg rPA, no Alum
4	5	Liquid, IM 10 μg rPA, Alum	Liquid, IM 10 μg rPA, no Alum
5	5	Liquid, IM 10 μg rPA, Alum	rPA Solid State Film (10% rPA)
6	5	Liquid, IM 10 μg rPA, Alum	SSBMS I (2.5% rPA)
7	5	Liquid, IM 10 μg rPA, Alum	SSBMS II (5% rPA)
8	5	Liquid, IM 10 μg rPA, Alum	SSBMS III (10% rPA)

whole blood, was stored at −80°C for later analysis of antibody levels. The animals received the second immunization in the form of one of the treatment groups listed in Table III on Day 28. Again, blood was drawn two weeks after immunization on Day 42 to assay the serum for IgG levels.

Anti-rPA IgG Antibody Assay

Serum anti-rPA IgG titers were measured by an enzyme-linked immunosorbent assay (ELISA). A 96-well flat bottom ELISA plate (Microlon, Greiner Labortechnik) was coated with 50 µl/well of either 3 µg/ml recombinant protective antigen for the test sera samples or 5 µg/ml rabbit anti-rat IgG capture antibody (Bethyl Laboratories, Montgomey, TX) for the rat serum IgG reference standards and then incubated for 2 h at 37°C. The plate wells were washed with phosphate-buffered saline containing 0.05% Tween buffer (PBS-T) and then blocked with PBS-T supplemented with 20% newborn calf serum (NBCS) (Hyclone Laboratories, Logan, UT) by incubating overnight at 4°C. The next day, the plate wells were washed again with PBS-T, and the test sera samples and IgG standards were diluted, as appropriate, with PBS-T + 10%NBCS for a total of 50 µl per well and incubated for 4 hrs at 37°C. The plate wells were washed with PBS-T and 50 µl of secondary antibody, 0.2 µg/ml horseradish peroxidase (HRP)-labeled rabbit anti-rat IgG (Bethyl) were added to each well and incubated for 2 h at 37°C. Anti-rPA IgG was then detected by adding 50 µl of HRP substrate (ABTS) and reading the absorbance of each well at 405 nm using a microplate reader (SpectraMax M5). The antibody titer was quantified using the calibration curve based on the reference IgG standard.

Transepidermal Water Loss Measurements

Transepidermal Water Loss (TEWL) was measured for each transdermal application site using the Vapometer™ (Delfin Technologies, Kuopio Finland). The device measures the rate of water evaporation from the skin and provides an indication of the integrity of the skin barrier. TEWL was measured before and immediately after the SSBMS treatments. If the baseline (before treatment) TEWL value was high (above 20 g/m^2/hr), an alternate administration site was selected.

Post-Application SSBMS Analysis

For both the *in vitro* and in *vivo* studies, the used SSBMS arrays were retained for microscopic inspection of the residual microstructures using a stereoscope equipped with a graticule in the eyepiece (Model SZ61, Olympus, Inc., Center Valley, PA). Arrays were mounted perpendicularly to the microscope objective so that the structures could be viewed from the side. Using the graticule, the heights of the residual microstructures were measured and compared with the original 200 µm height. The percentage of the remaining microstructure length in eight representative microstructures and the percentage of the SSBMS array area showing dissolution were recorded. The two metrics allowed the estimation of the amount of FITC-BSA or rPA delivered into the skin based on a geometric calculation of the total volume of the dissolved portion of the pyramid-shaped microstructures and the protein contents of the formulations.

Statistical Analysis

Mean values reported in this study represent the average of at least five replicates. Error bars are the standard deviations of the means (SD). When a comparison between two means was required, a Student's *t*-test with a 95% level of confidence ($\alpha = 0.05$) was used. Comparisons between two or more means were performed using a one-way analysis of variance at the same level of confidence (ANOVA, $\alpha = 0.05$). A p-value < 0.05 was considered to indicate statistical significance.

RESULTS

FITC-BSA *In Vitro* Skin Delivery

Fig. 2 shows a microscopic view of an array of SSBMS arrays containing FITC-BSA under UV excitation. The location of fluorescence within the microstructures corresponds to the localization of the protein within the microstructures. To determine whether the MicroCor platform could be used to deliver macromolecules transdermally, these FITC-BSA SSBMS arrays were first tested *in vitro* using human cadaver skin. FITC-BSA permitted the use of

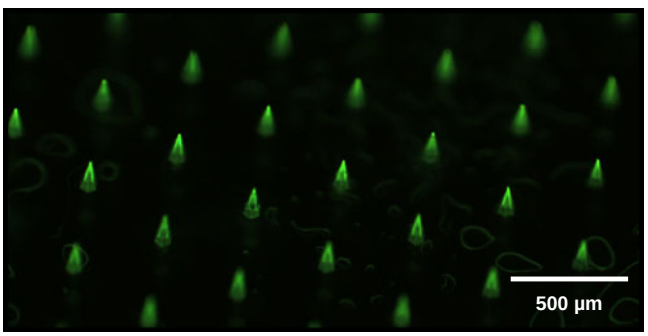

Fig. 2 Representative fluorescence image of solid-state biodegradable microstructures (SSBMS) containing FITC-labeled bovine serum albumin. [Scale: center-to-center spacing = 400 µm].

fluorescence to visualize and quantify the amount of protein within the SSBMS and the skin.

FITC-BSA SSBMS arrays were applied to human cadaver skin for 2 min using a custom-made spring-loaded impactor. Fig. 3 shows representative images of microstructure penetration into the skin using both (A) light and (B) fluorescence (UV excitation) microscopy. The individual microstructure penetrations are especially visible with fluorescence microscopy and show excellent skin penetration efficiency, i.e., uniform penetration over the entire array area.

After application, the used SSBMS arrays were inspected under a microscope to evaluate and measure the heights of the residual microstructures. Fig. 4 shows representative photos of a SSBMS array containing FITC-BSA before application and the same array after skin penetration. The almost complete dissolution of the microstructures can clearly be seen. For all of the FITC-BSA SSBMS arrays tested in this study, dissolution of the microstructures was observed over >95% of the entire array area, and the length of the microstructures dissolved was >75% of the original 200 μm length.

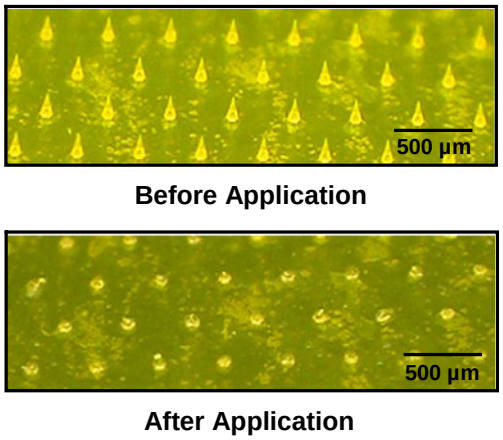

Fig. 4 Representative light microscopy images of a FITC-BSA-containing SSBMS array before and after application to human cadaver skin *in vitro*. Microstructures are almost fully dissolved.

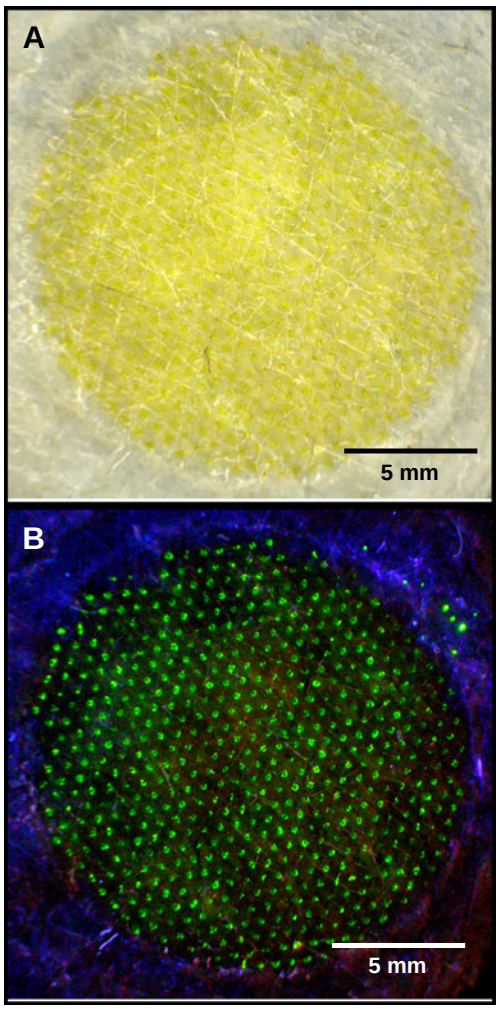

Fig. 3 Representative image of FITC-BSA delivery within human cadaver skin after treatment with a SSBMS array. Microstructure penetrations can be seen with a stereoscope under both light (**a**) and UV-excited fluorescence (**b**) microscopy conditions.

To quantify the amount of FITC-BSA delivered *in vitro*, the FITC-BSA was extracted from the skin and analyzed. The surface of each skin sample was tape-stripped to ensure that the BSA extracted was not simply adsorbed to the skin surface. Fig. 5 shows the total amount of FITC-BSA extracted from the human cadaver skin after treatment with SSBMS arrays made from two FITC-BSA formulations (A and B). Formulation A arrays (5% FITC-BSA) delivered 12.0±1.3 μg FITC-BSA into the skin, while Formulation B arrays (10% FITC-BSA), which contained twice as much FITC-BSA, delivered almost twice as much

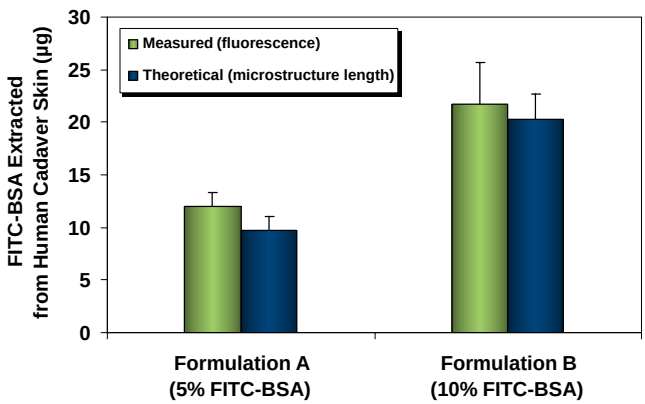

Fig. 5 Measured and theoretical *in vitro* FITC-BSA delivery to human cadaver skin after treatment with Formulations A and B, which contain 5% and 10% w/w FITC-BSA, respectively. Measured values were determined by extraction of FITC-BSA from excised skin. Theoretical values were estimated based on the residual length of the microstructures after penetration. ($n = 8$ per formulation).

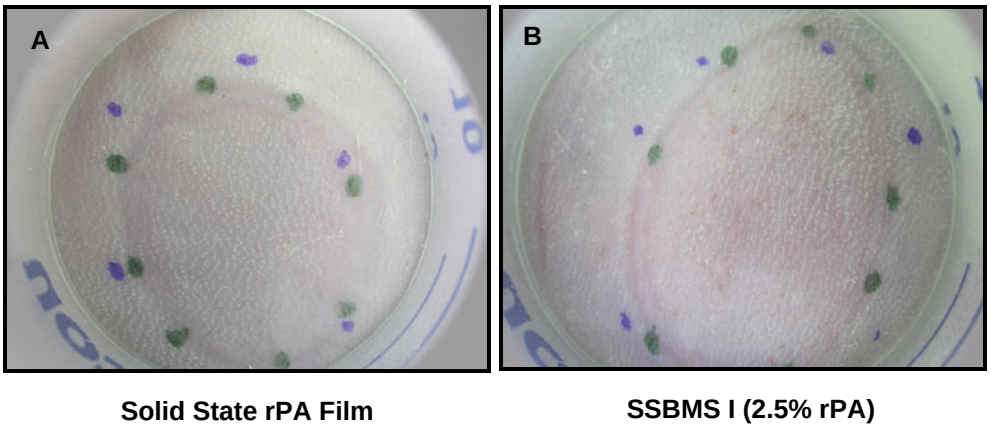

Fig. 6 Representative photographs of skin sites after *in vivo* application of the solid-state rPA film and an rPA-containing SSBMS array in the rat model. Note: Treatment sites have been outlined with blue and green marker. The microstructures were well tolerated, as evidenced by the lack of edema and the no-more-than-mild erythema.

FITC-BSA, 21.7±4.0 μg. FITC-BSA removed by tape stripping accounted for less than 7% of the total FITC-BSA extracted from the skin and tape combined (data not shown). Fig. 5 also shows that the theoretical FITC-BSA delivery (9.7±1.3 μg and 20.3±2.4 μg FITC-BSA for Formulations A and B arrays, respectively) calculated based on the observed length of microstructure remaining and the percentage of the array area showing dissolution were comparable to the experimentally measured delivery.

rPA Delivery and Immunogenicity Study

Local Skin Tolerability

After administration of the rPA-containing SSBMS arrays and the solid-state film, there was no observable edema on any of the 20 treatment sites (all scores=0), and erythema ranged from none (score=0) to slight (score=1) for both the film treatments and the array treatments. The average erythema score for the four treatments was 0.6±0.5 for the film, 1.0±0.0 for SSBMS I, 0.6±0.5 for SSBMS II, and 0.8±0.4 for SSBMS III. The fact that there was no statistically significant difference in erythema between the film and the SSBMS arrays (p=0.46; one-way ANOVA) suggests that the method of application, i.e., the high velocity impactor, is likely a major influence on the development of erythema. Although small numbers of petechiae were visible at many of the SSBMS application sites, light blotting of the skin revealed no blood on the skin surface. Fig. 6 shows representative images of the rat skin after application of the solid-state film and a SSBMS array (2.5% rPA formulation) transdermal treatment.

Transepidermal Water Loss

TEWL was measured before and after transdermal applications to assess whether the microstructures penetrated the skin, thus causing an increase in the skin's water evaporation rate. The average of the TEWL for each transdermal group before and after treatment is summarized in Table IV. For the three SSBMS transdermal groups, there was a significant increase in the TEWL after treatment when compared to the baseline values measured before treatment (p-values for each group≤0.002). For the solid-state film group there was essentially no change in TEWL (p-value=0.81), which is consistent with the absence of microstructures.

SSBMS Dissolution

When the used SSBMS arrays, which had been applied to skin for 2 min, for each treatment group were inspected under the microscope, all arrays showed good dissolution over >95% of the array area (data not shown). Table V

Table IV TEWL Values for Skin Sites Measured Before and After Transdermal Applications

Treatment Group	TEWL (g/m^2-hr)		TEWL Ratio (After/Before)
	Before Treatment	After Treatment	
SSBMS I (2.5% rPA)	10.6±2.5	28.1±2.8	2.8±0.78
SSBMS II (5% rPA)	6.7±0.2	22.1±2.1	3.3±0.36
SSBMS III (10% rPA)	11.0±2.4	22.1±4.2	2.1±0.43
Solid State Film (10% rPA)	7.4±1.9	7.6±2.1	1.1±0.25

Table V Residual Microstructure Lengths and Estimated rPA Delivery after SSBMS Treatments

Treatment Group	Microstructure Length Remaining (μm)	Estimated rPA Delivery (μg)
SSBMS I (2.5% rPA)	43.4 ± 18.1	5.1 ± 1.6
SSBMS II (5% rPA)	45.6 ± 20.5	9.8 ± 3.3
SSBMS III (10% rPA)	48.4 ± 8.8	18.0 ± 3.3

shows that the average microstructure length dissolved, i.e., >75% of the 200 μm length, was approximately the same for the three SSBMS groups (one-way ANOVA, $p=0.89$). Since the extent of dissolution was similar for the three different formulations, estimates of rPA delivery based on the microstructure length remaining correlated with the rPA content in the original formulations. As the rPA content increased by a factor of two for the three formulations, so too did the rPA delivery, e.g., 5.1 μg for 2.5% rPA, 9.8 μg for 5% rPA, and 18.0 μg for 10% rPA.

IgG Antibody Titers after Immunization

Fig. 7 shows the anti-rPA antibody titers for the individual animals in each treatment group. The estimated amounts of rPA delivered rounded to the nearest microgram are reported in parentheses for the immunization treatments. All groups received the same primary immunization, and, as expected and as shown in Fig. 7a, the antibody titers at 2 weeks post primary immunization were comparable for all eight treatment groups ($p=0.31$). After the second immunization, there were several differences seen among the various groups, with results depicted in Fig. 7b.

An increase in antibody titer was observed for the control (none) group after the second two-week period even with no second immunization. The increase was likely due to the presence of the alum adjuvant in the initial immunization, which may have caused the primary immune response period to be extended. Nevertheless, antibody titers for the 10 μg ID and IM treatment groups, though not statistically different from each other ($p=0.88$), were higher than the control ($p=0.001$ and 0.009, respectively) and the solid-state film groups ($p=0.007$ and 0.03, respectively). Likewise, the transdermal SSBMS II (10 μg) and SSBMS III (18 μg) groups had significantly higher antibody titers than the control (none) and solid-state film (all $p<0.0001$). The transdermal SSBMS II and SSBMS III groups also had statistically higher antibody titers than the ID (10 μg) group ($p=0.04$ and 0.03, respectively) and higher, but not statistically different, IgG titers than the IM (10 μg) group ($p=0.09$ and 0.07, respectively), due to the higher variability seen in the IM group. The antibody titers were comparable for transdermal SSBMS II (10 μg) and SSBMS III (18 μg) groups, suggesting a plateau in the dose-response curve above a certain threshold antigen concentration ($p=0.73$).

The transdermal 5 μg SSBMS I group had antibody titers that were significantly lower than both the SSBMS II and SSBMS III groups ($p<0.0001$). Instead, the group was comparable to the 1 μg ID group and the solid-state film ($p=0.39$ and 0.98, respectively), suggesting a minimal threshold concentration required for eliciting an increase in the IgG response (typical of an S-shaped dose response curve). The 5 μg SSBMS I group was expected to have a higher titer based on the robust response of the 10 μg SSBMS II group. However, our doses for the transdermal SSBMS groups are indirect estimates based on microscopic evaluation of microstructure dissolution, and, as a result, there could be some error with these dose estimations.

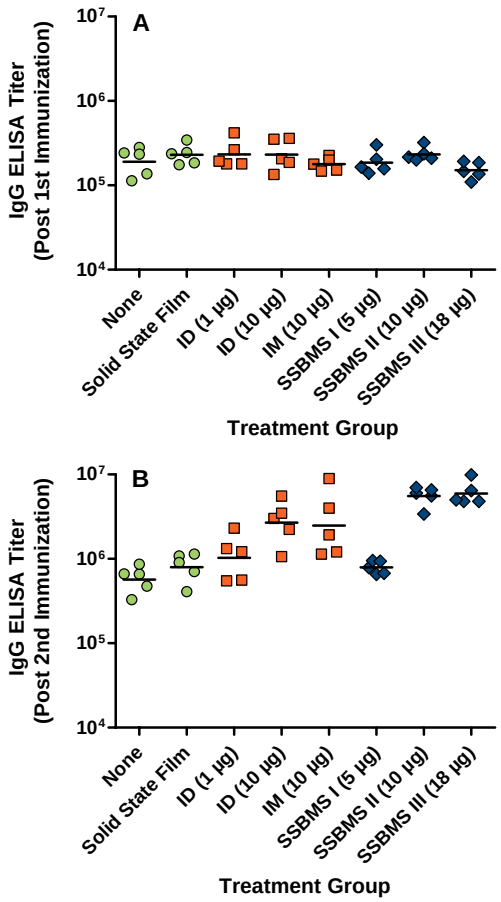

Fig. 7 Individual serum anti-rPA IgG antibody titers measured two weeks after the first immunization (**a**) and two weeks after the second immunization (**b**) for each treatment group. Geometric means are also plotted for each treatment group. The estimated amount of rPA delivered is reported in parentheses for immunization groups.

DISCUSSION

The transdermal route is a well-accepted route of administration as is evident from patient acceptability and the commercial success of patches in several therapeutic areas, e.g., pain management, hormone replacement, nicotine cessation, hypertension and Alzheimer's. The transdermal route is limited, however, to small molecule delivery due to the excellent barrier properties of the skin. The surge in development of biotechnologically based macromolecule drugs and a renewed interest in vaccines have created an opportunity for the development of needle-free transdermal delivery systems for painless, safe and effective delivery of these drugs.

Evaluations of the microstructures after both *in vitro* and *in vivo* skin penetration indicate that rapid dissolution (within 2 min) and penetration depths of at least 100 μm, and possibly more than 150 μm, can be achieved. At this depth, the skin irritation effects observed in rats were mild and transient. The FITC-BSA *in vitro* delivery results demonstrated that uniform penetration and dissolution of the microstructures can also be achieved. The almost complete dissolution of the microstructures also highlights an important safety feature of the technology. Once the microstructures have dissolved within the skin, there is minimal risk of accidental reapplication, and disposal of sharps will be less of an issue.

The immune response expressed in terms of anti-rPA titers, which has been shown to be a good indicator of overall protective immunity [10], was higher after transdermal delivery of rPA with the SSBMS than after the ID and IM routes of administration. Also, the immune response after transdermal delivery with the SSBMS was more consistent and reproducible as compared to the ID and IM routes of delivery. Interestingly, there was no statistical difference observed between the 10 μg IM and ID groups in this study. In some literature reports, the ID route has been shown to have a better antibody response than the IM route for certain antigens, although this may not always be the case [11–13]. The overall improved response seen with the transdermal route *versus* traditional injections may indicate that different aspects of the immune system are responsible for the anti-rPA antibody response, and it is possible that the balance of antigen presentation by dermal dendritic cells in the dermis and/or Langerhans cells in the epidermis determine the overall antibody response.

CONCLUSIONS

In this study, we have demonstrated the feasibility of using solid-state biodegradable microstructures for safe and effective delivery of macromolecules. The technology can be used to effectively penetrate the outer layers of the skin to deliver large drug molecules in a rapid fashion for both local and systemic uptake. The next steps are to leverage the MicroCor technology to develop therapeutic drug/vaccine candidates that are cost-effective and amenable to commercial scale-up.

ACKNOWLEDGMENTS

The authors would like to acknowledge Appala Sagi, Danir Bairamov, Mikhail Shapiro, Creag Trautman, and Wade Worsham of Corium International, Inc. for fabrication of the SSBMS arrays and design of the custom impactor device. The authors would also like to gratefully acknowledge Raymond Daynes of the University of Utah for helpful discussions and technical assistance with executing the immunization studies.

REFERENCES

1. Prausnitz MR. Microneedles for transdermal drug delivery. Adv Drug Deliv Rev. 2004;56:581–7.
2. McAllister DV, Wang PM, Davis SP, Park JH, Canatella PJ, Allen MG, *et al.* Microfabricated needles for transdermal delivery of macromolecules and nanoparticles: Fabrication methods and transport studies. Proc Natl Acad Sci U S A. 2003;100:13755–60.
3. Matriano JA, Cormier M, Johnson J, Young WA, Buttery M, Nyam K, *et al.* Macroflux microprojection array patch technology: A new and efficient approach for intracutaneous immunization. Pharm Res. 2002;19:63–70.
4. Wang PM, Cornwell M, Hill J, Prausnitz MR. Precise microinjection into skin using hollow microneedles. J Invest Dermatol. 2006;126:1080–7.
5. Xie Y, Xu B, Gao Y. Controlled transdermal delivery of model drug compounds by MEMS microneedle array. Nanomedicine. 2005;1:184–90.
6. Teo MA, Shearwood C, Ng KC, Lu J, Moochhala S. *In vitro* and *in vivo* characterization of MEMS microneedles. Biomed Microdevices. 2005;7:47–52.
7. Rajaraman S, Henderson HT, Rajaraman S, Henderson HT. A unique fabrication approach for microneedles using coherent porous silicon technology. Sens Actuators B Chem. 2005;105:443–8.
8. Zahn JD, Deshmukh A, Pisano AP, Liepmann D. Continuous on-chip micropumping for microneedle enhanced drug delivery. Biomed Microdevices. 2004;6:183–90.
9. Draize JH. Methods for the study of irritation and toxicity of substances applied topically to the skin and mucous membranes. J Pharmacol Exp Ther. 1944;83:377–90.
10. Little SF, Ivins BE, Fellows PF, Pitt ML, Norris SL, Andrews GP. Defining a serological correlate of protection in rabbits for a recombinant anthrax vaccine. Vaccine. 2004;22:422–30.
11. Henderson EA, Louie TJ, Ramotar K, Ledgerwood D, Hope KM, Kennedy A. Comparison of higher-dose intradermal hepatitis B vaccination to standard intramuscular vaccination of healthcare workers. Infect Control Hosp Epidemiol. 2000;21:264–9.
12. Alarcon JB, Hartley AW, Harvey NG, Mikszta JA. Preclinical evaluation of microneedle technology for intradermal delivery of influenza vaccines. Clin Vaccine Immunol. 2007;14:375–81.
13. Belshe RB, Newman FK, Wilkins K, Graham IL, Babusis E, Ewell M, *et al.* Comparative immunogenicity of trivalent influenza vaccine administered by intradermal or intramuscular route in healthy adults. Vaccine. 2007;25:6755–63.